

Negative fire feedback in a transitional forest of southeastern Amazonia

JENNIFER K. BALCH*, DANIEL C. NEPSTAD†‡, PAULO M. BRANDO‡§, LISA M. CURRAN*, OSVALDO PORTELA‡, OSWALDO DE CARVALHO JR‡¶ and PAUL LEFEBVRE†
*School of Forestry and Environmental Studies, Yale University, 370 Prospect Street, New Haven, CT 06511, USA, †Woods Hole Research Center, 149 Woods Hole Road, Falmouth, MA 02450, USA, ‡Instituto de Pesquisa Ambiental da Amazônia, Av. Nazaré 669, 66035-170 Belém, Brazil, §Department of Botany, University of Florida, PO Box 118526, Gainesville, FL 32611, USA, ¶Durrell Institute of Conservation and Ecology, University of Kent, Canterbury, Kent CT2 7NR, UK

Abstract

Anthropogenic understory fires affect large areas of tropical forest, particularly during severe droughts. Yet, the mechanisms that control tropical forests' susceptibility to fire remain ambiguous. We tested the widely accepted hypothesis that Amazon forest fires increase susceptibility to further burning by conducting a 150 ha fire experiment in a closed-canopy forest near the southeastern Amazon forest–savanna boundary. Forest flammability and its possible determinants were measured in adjacent 50 ha forest plots that were burned annually for 3 consecutive years (B3), once (B1), and not at all (B0). Contrary to expectation, an annual burning regime led to a decline in forest flammability during the third burn. Microclimate conditions were more favorable compared with the first burn (i.e. vapor pressure deficit increased and litter moisture decreased), yet flame heights declined and burned area halved. A slight decline in fine fuels after the second burn appears to have limited fire spread and intensity. Supporting this conclusion, fire spread rates doubled and burned area increased fivefold in B3 subplots that received fine fuel additions. Slow replacement of surface fine fuels in this forest may be explained by (i) low leaf litter production ($4.3 \text{ Mg ha}^{-1} \text{ yr}^{-1}$), half that of other Amazon forests; and (ii) low fire-induced tree and liana mortality ($5.5 \pm 0.5\% \text{ yr}^{-1}$, SE, in B3), the lowest measured in closed-canopy Amazonian forests. In this transitional forest, where severe seasonal drought removed moisture constraints on fire propagation, a lack of fine fuels inhibited the intensity and spread of recurrent fire in a negative feedback. This reduction in flammability, however, may be short-lived if delayed tree mortality or treefall increases surface fuels in future years. This study highlights that understanding fuel input rate and timing relative to fire frequency is fundamental to predicting transitional forest flammability – which has important implications for carbon emissions and potential replacement by scrub vegetation.

Keywords: Brazilian Amazon, carbon emissions, feedbacks, fire ecology, forest–savanna transitions, fuel, large-scale experimental burns, Mato Grosso transitional forests, tropical forests, tropical wildfires

Received 4 December 2007; revised version received 27 February 2008 and accepted 26 March 2008

Introduction

Understory wildfire in closed-canopy tropical forests causes substantial carbon emissions and is a potential catalyst of forest degradation and substitution. During the 1997–98 droughts, related to the El Niño–Southern

Oscillation (ENSO), understory wildfires burned 39 000 km² of Amazon forests, twice the average area deforested annually in Brazil from 1988 to 2005 (INPE, 2006), and committed 0.024–0.165 PgC to the atmosphere (Alencar *et al.*, 2006). Fire could have a more lasting effect on the global carbon budget if vegetation change ensues. Currently, the extent of closed-canopy forest is suppressed by fire in South America and Africa and would double in a modeled no-fire world, repla-

Correspondence: Jennifer K. Balch, tel. +1 202 360 0923, e-mail: jennifer.balch@yale.edu

cing savanna or grassland (Bond *et al.*, 2005). Although charcoal deposits throughout the Amazon suggest that fire has affected neotropical forests at multiple-century intervals over the past few millennia (Sanford *et al.*, 1985; Hammond *et al.*, 2007), increasing fire frequency associated with human land use is expected to shift forests to savanna-like or scrub vegetation (Cochrane *et al.*, 2004). Moreover, Amazon savanna–forest boundaries are expected to be sensitive to fire regime and climate shifts (Ratter, 1992; Grogan & Galvão, 2006).

The Amazon's transitional forests (approximately 400 000 km²) lie between the 2-million km² *cerrado*, or savanna, of central Brazil to the south and more humid forests to the north. Transitional forests differ from dense, tall forests to the north in their shorter stature (mean canopy height: 20 ± 1, SE, m), lower leaf area index (LAI maximum: 5 m² m⁻²), and lower above-ground biomass (191 ± 6, SE, Mg ha⁻¹) (see 'Materials and methods'). Although half of Amazon forests experience seasonal drought, when average daily rainfall is <1.5 mm during the driest 3 months (Nepstad *et al.*, 1994), intensity of seasonality increases close to the southern forest–savanna border (Sombroek, 2001). At our field site, in the Brazilian state of Mato Grosso, total annual rainfall is 1739 mm yr⁻¹, but there is a severe dry season from May to September, when rainfall is <10 mm month⁻¹ for 3 months followed by <50 mm month⁻¹ for 2 months.

In addition to severe annual drought, these transitional forests currently incur some of the highest deforestation rates in Brazil due to soy and cattle pasture expansion (INPE, 2006; Morton *et al.*, 2006; Soares-Filho *et al.*, 2006), and are consequently exposed to anthropogenic ignition sources (Alencar *et al.*, 2004). The prediction of climate-driven dieback of closed-canopy forests in the Amazon toward the end of the 21st century (Oyama & Nobre, 2003; Cox *et al.*, 2004; Hutyra *et al.*, 2005) – which would substantially shift the forest–savanna boundary – may be superseded or exacerbated by fire-driven changes in Amazon forests. During the 2001 ENSO-related drought, a third of Amazon forests were susceptible to fire due to soil moisture depletion, and the entire southeastern transitional forest formation was at high fire risk (Nepstad *et al.*, 2004). Yet, there is currently insufficient understanding of transitional forests and their response to increasing understory fire frequency to predict the future trajectory of this vulnerable forest (Rodríguez *et al.*, 2007).

It was hypothesized that understory wildfire increases the flammability of seasonally dry Amazon forests by killing trees, causing greater sunlight penetration into the forest interior, faster drying of the fuel layer, and additional surface fuel build-up (Nepstad *et al.*, 1995, 1999). Indeed, canopy height and density

were associated with the spread rates of experimental fires in a central Amazon forest and both decline following fire (Ray *et al.*, 2005). Moreover, fires were found to burn more intensely in eastern Amazon forests that had been previously burned (Cochrane & Schulze, 1999; Cochrane *et al.*, 1999), and prior disturbance from logging and fire was the best predictor of fire occurrence in another eastern Amazon landscape (Alencar *et al.*, 2004).

Microclimate and fuel moisture – rather than fuel mass – control fire behavior in seasonally dry, evergreen Amazon forests where 75% of the 2000 mm of yearly rainfall comes during the 6-month wet season (Nepstad *et al.*, 2002; Ray *et al.*, 2005). However, in seasonal, but drier Bolivian semideciduous forests (1500 mm yr⁻¹), total canopy cover had little influence on whether experimental forest plots burned (Blate, 2005). During the severe dry season in Amazon transitional forests, fuel loads may have a greater effect on fire intensity and spread than understory moisture dynamics. This may explain why Amazon transitional forests are susceptible to fire during both normal and drought years, whereas moist forests burn more during ENSO-related droughts (Alencar *et al.*, 2006). Understanding what controls fuel stocks and replacement may be essential for assessing fire probability and modeling carbon emissions from understory transitional forest wildfires. Yet, few experimental, field-based studies exist that test the controls of fire behavior or document fuel load trajectories with initial or repeat fires in these forests.

Therefore, we established a 150 ha burn experiment within Amazon transitional forests, 30 km north of the forest–*cerrado* boundary. The scale at which wildfires occur in the Amazon requires a large-scale ecosystem approach, which makes adequate experimental replication challenging (Oksanen, 2001). A necessary limitation of this experiment is that we treat sampling within the 50 ha treatment plots as independent, which we acknowledge as a form of pseudoreplication that is often associated with experimental fires (van Mantgem *et al.*, 2001). Key advantages of our planned burns, however, are that we were able to conduct intensive pre-, during-, and postfire measures and compare with an unburned control, following well-established procedures for large experimental manipulations without true replication (Hurlbert, 1984).

The objectives of the first 2 years of this experiment were threefold. First, we determined the effect of fire history on forest flammability (defined by the proportion of burned forest floor and flame heights) by comparing possible determinants of fire behavior [fuel load, fuel moisture, and air vapor pressure deficit (VPD)] within a previously once-burned (B1) and twice-burned (B3) plot, compared with a control (B0). Second, we

tested the hypothesis that fuel becomes limiting to fire following consecutive annual burns by comparing fire behavior in twice-burned forest subplots (in B3 plot) with and without fine fuel additions. Third, we documented fuel combustion loss from our prescribed burns in order to provide necessary, but lacking, field-based estimates of carbon emissions from tropical understory fires.

Materials and methods

Site description

The study site is located on Fazenda Tanguro, a privately owned farm 75 km north of Canarana, in the Brazilian state of Mato Grosso, in the southern part of the Amazon basin ($13^{\circ}04'35.39''\text{S}$, $52^{\circ}23'08.85''\text{W}$; Fig. 1). The experimental forests are found within the region's remaining transitional forest formation, and are lower in diversity [97 tree and liana species ≥ 10 cm diameter at breast height (DBH)] than more humid, northern forests. Furthermore, nine species represent 50% of the Importance Value Index (IVI), with a prevalence of Lauraceae and Burseraceae (Supplementary Information-Appendix S1). Soils are Oxisols (Haplustox) with a water table at 12–15 m depth and no impeding layers.

Precipitation, temperature, and relative humidity

A meteorological station, <1 km from the forest plots, was established in an open area to measure temperature (T , $^{\circ}\text{C}$) and relative humidity (RH, %) during the study period (starting July 2004). A pair of Hobo RH-T sensors were used to log readings at 30 min intervals (Onset Computer Corporation, Pocasset, MA, USA). Dry-season T was 25°C and RH was 66% (average daily values used to calculate). Rainfall was monitored from July 2004 to February 2006 with an automated pluviometer (RainWise 20 cm diameter tipping-bucket; RainWise Inc., Bar Harbor, ME, USA). Mean precipitation, 1739 mm yr^{-1} , during both study years was not anomalous when compared with the prior 8 years of rainfall data collected by the farm (T. Ranch, unpublished data). In addition, 35 Hobo RH-T sensors, placed at randomly selected grid points and rotated biweekly, measured T and RH at 30 min intervals in the forest understory. Maximum daily August VPD was defined as the 0.75 quantile of the VPD values recorded over a 24 h period.

Study design

One $1.5\text{ km} \times 1.0\text{ km}$ (150 ha) experimental plot with three treatment plots ($0.5\text{ km} \times 1.0\text{ km}$, 50 ha) was established in the property's legally protected forest reserves

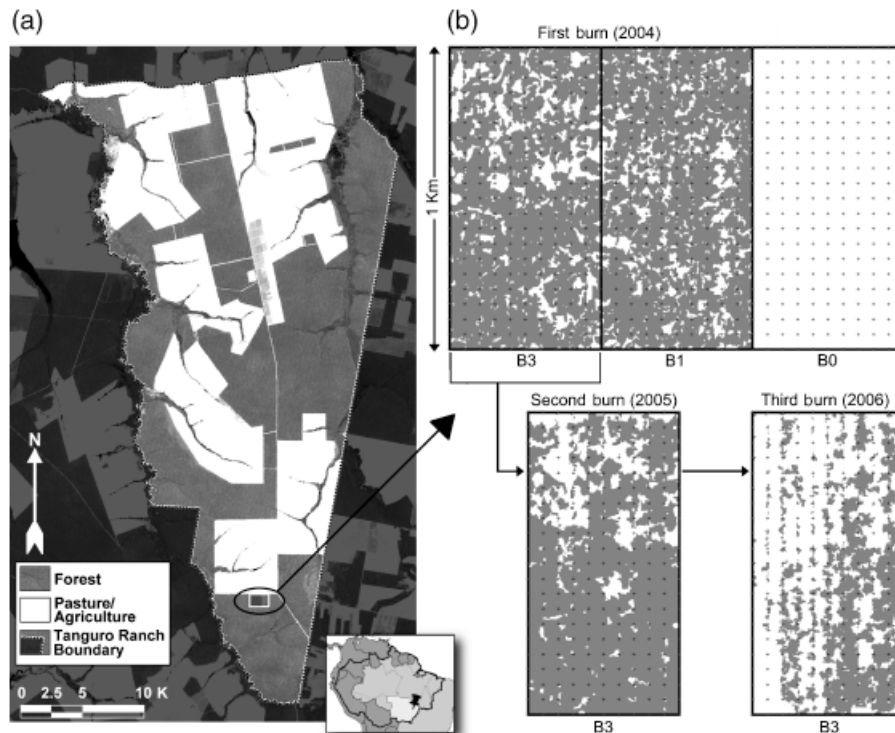


Fig. 1 (a) Location of experimental plot on Tanguro Ranch. Inset map shows study site located in Mato Grosso state, in the Amazon basin. (b) Burn pattern in once-burned (B1) and annually burned (B3) 50 ha plots from three consecutive prescribed fires (burned areas in gray, unburned in white).

(Fig. 1). Location was selected along a pasture edge within forest without logging or previous fire, with <2% slope, and containing ≥ 1000 m of forest extending around the experimental block. Three 50 ha treatment plots within the block include a control (B0), a plot burned once in 3 years (B1), and a plot burned three times in 3 years (B3). Trails (1 km) were cut in a N–S direction every 50 m with nine perpendicular trails (1.5 km) at varying distances from the edge.

Aboveground biomass, canopy height, and canopy density

In each 50 ha treatment plot, we tagged, mapped, and measured height (m) and DBH (at 1.3 m) of all trees ≥ 40 cm DBH ($N \sim 930$ individuals per plot). Trees and lianas (≥ 20 cm DBH) were sampled in belt transects (500 m \times 20 m) at 0, 30, 100, 250, 500, and 750 m from the edge (5.5 ha sampled per treatment plot; $N \sim 880$ individuals per plot). Nested sub-sampling of trees and lianas 10–19.9 cm DBH occurred within the same belt transects (500 m \times 4 m; 1.2 ha sampled per treatment plot; $N \sim 490$ individuals per plot). All sampled trees and lianas were identified to species. This floristic inventory was used to calculate IVI for the overall experimental plot and each treatment plot before burning (Supplementary Information – Appendix S1). Tree height was measured using a clinometer.

Using height and DBH measurements, aboveground biomass for trees was calculated with allometric equations developed for tropical moist forests with a marked 1–4 month dry season and annual precipitation between 1500 and 3500 mm yr⁻¹ (Chave *et al.*, 2005); for lianas, basal diameter was used to calculate biomass from a diameter-based allometric equation (Gerwing & Farias, 2000). Our estimate of aboveground biomass for trees and lianas ≥ 10 cm DBH, 191 ± 6 (SE) Mg ha⁻¹, was calculated by plot ($N = 3$). Also, our estimate of mean canopy height, 20 ± 1 (SE) m, was calculated using all trees ≥ 20 cm DBH and then averaged by plot ($N = 3$).

LAI was measured three times during the experiment – May 2005, August 2005, and July 2006 – at 50 m intervals on all N–S trails ($N = 230$ per treatment plot) using two LiCor-2000 Plant Canopy Analyzers in differential mode (LI-COR Inc., Lincoln, NE, USA; Welles, 1990). One instrument was placed in an adjacent open field to measure incoming radiation with no canopy influence; the other was simultaneously used to take understory measurements. The instruments were inter-calibrated before each set of measurements in the open field. The light field of each sensor was reduced to 90° using opaque sensor caps. Measurements were taken during diffuse light conditions – either before 8:00 or after 17:00 hours. LAI calculations were made using the inner four quantum sensor rings.

Experimental burns

Three annual experimental burns were conducted near the end of the dry season, when many escaped wildfires occur. The first experimental fire was set in both B1 and B3 plots in August 2004. The second and third burns were set in plot B3 in September 2005 and August 2006. More than 2 months of rainless days preceded the 2004 and 2006 burns. In 2005, 4.3 mm of rain fell 11 days before burning; this was the total precipitation over the preceding 2 months. During each consecutive burn, mean (\pm SE) daily T , measured at the meteorological station, was 24.0 °C (± 0.5 °C), 28.7 °C (± 0.1 °C), and 27.6 °C (± 0.7 °C). Also, mean daily (\pm SE) RH was 51% ($\pm 2\%$), 57% ($\pm 1\%$), and 55% ($\pm 1\%$) during the first, second, and third burns, respectively. Wind speed was low in the understory (< 0.5 m s⁻¹) and had little noticeable effect on fire behavior during all years. Before the firelines were set, we also measured T and RH at 25 m intervals along the forest floor using battery-powered psychrometers.

Fires were set with kerosene drip torches along the N–S trails; a total of 10 km of firelines were set per plot during 3–4 consecutive days between 9:00 and 16:00 hours. During all years, fires extinguished at night (likely due to low VPD) and were relit on subsequent days. The spatial burn pattern was then mapped on a 5 m \times 5 m scale within a month postfire (Fig. 1). A limitation of this study is that the experimental fires may not replicate the actual fire intensity, spread rate, and burn pattern of accidental fires that move into the understory from adjacent land use. Ignition sources were likely twice that found in an escaping wildfire, where a single fireline moves in from a forest edge. Here, within each 50 m \times 50 m cell, two parallel firelines advance from trails on either side. Also, accidental fires often occur under distinct weather conditions (e.g. high surface winds) and, as a result, may have higher fire intensities and faster spread rates than the prescribed fires of this experiment.

During the burns flame height and width, fire spread rate (FSR), and flame T were measured. Flame heights and widths were measured at 25–50 m along the advancing fireline. FSR was calculated by visiting these same reference points and noting distance spread between time intervals. Maximum flame T at the surface and maximum soil T at 2 cm belowground were measured using Tempilaq heat sensitive paints (range: 79–1093 °C) with an interval between paints of 56 °C. These paints were applied to a copper plate and placed at 2 cm below ground and at ground level.

To test whether flame heights, widths, and VPD differed with increasing fire frequency, one-way analysis of variance was used with Tukey's HSD contrasts to identify significant differences in mean values.

Mortality rate and standing dead fuels

All inventoried trees were censused annually immediately before that year's prescribed burns. Mortality was designated if all aboveground tissue was dead (a stem was also considered dead if only live basal sprouts were present). Annual mortality rate (m) was calculated as follows:

$$m = 1 - \left(1 - \frac{D}{N}\right)^{1/t},$$

where N is the initial number of live stems, D is the number of dead stems at the end of the measurement interval, and t is the time interval between surveys measured in years (Sheil & May, 1996).

Standing dead fuels were measured pre- and postfire in the same transects for 10–19.9 cm DBH and ≥ 20 cm DBH stems ($N = 6$ per treatment plot). DBH and height (m) of standing dead stems were measured to calculate volume, which was then multiplied by an estimate of the specific gravity of sound wood, 0.69 g cm^{-3} (Brown & Lugo, 1992), to obtain biomass. Where height data were missing, heights were underestimated at 2 m (the minimum height to enter as a standing dead stem). Logistic regression was conducted to determine whether the probability of combustion of standing dead stems increased with repeated burns in the B3 plot.

Fuel measurements

Within a week pre- and postfire, downed woody fuel loads were measured using Brown's planar transect method ($N = 27$ per treatment plot; Brown *et al.*, 1982). Based on diameter, downed woody debris was partitioned by standard fuel moisture timelag classes (Deeming *et al.*, 1977). Downed woody fuels, 1 h (0–0.6 cm diameter), 10 h (0.6–2.5 cm diameter), and 100 h (2.5–7.6 cm diameter), were counted that cross 2, 3, and 5 m planar transects, respectively. Fuels > 7.6 cm diameter, or 1000 h fuels, were counted and their diameters measured along a 10 m transect. Their condition (sound or rotten) was noted. Downed woody fuel biomass (Mg ha^{-1}) was calculated by multiplying the fuel volume by a wood density estimate; 0.69 and 0.52 g cm^{-3} , were used for sound and rotten wood, respectively. Leaf litter was collected within a 40 cm diameter wire circle at three points along the same 10 m transect. Concurrent with psychrometer measurements, leaf litter samples were collected before firelines in order to measure LMC (litter moisture content). Litter samples were oven-dried (65°C for 48 h), weighed, and averaged per transect. To calculate total necromass, total downed fuels were combined with total standing dead fuels by transect.

Analysis of covariance was used to test for differences in fuel loads among treatment plots 2 years after the initial burn treatment. Baseline fuels were accounted for as a covariate when necessary and Kruskal–Wallis tests used when analysis of variance assumptions were violated in certain fuel size classes. To test whether fuel consumption differed with repeated burns, linear mixed-effects modeling was used to first test for effects of repeated measures; if no repeated measure problems existed, then analysis of variance was conducted (with plots B1 and B3 joined for 2004 initial prescribed burn). If analysis of variance assumptions were violated, then Kruskal–Wallis tests were used. Also, Kruskal–Wallis test was applied to compare LMC values across years.

Litterfall

Litterfall was collected biweekly for 2 years (August 2004–August 2006) from 0.5 m^2 screened traps ($N = 90$ per treatment plot) placed systematically throughout the plots. Traps were suspended ~ 1 m above the forest floor. Following standard practice, woody debris (> 1 cm) was excluded (Clark *et al.*, 2001). Leaf litter was then oven-dried (65°C for 48 h) and weighed to calculate dry mass. Daily litterfall production was calculated by dividing dry mass by days between collections. To test whether annual litterfall differed across plots and with repeated burns linear mixed-effects modeling was used to first test for effects of repeated measures, if no repeated measure problems existed, then analysis of variance was conducted with contrasts.

Fuel additions in canopy gaps and nongaps

Adjacent canopy gaps (at least $25 \text{ m} \times 25 \text{ m}$ in size) and nongaps were identified within areas that had previously burned twice in the B3 plot. Nine ($50 \text{ m} \times 25 \text{ m}$) plots were then established within a randomly selected subset of these suitable areas. The plots were established where half ($25 \text{ m} \times 25 \text{ m}$) fell within a treefall gap and half within a closed-canopy area. LAI was measured at eight points within each of these subplots ($25 \text{ m} \times 25 \text{ m}$). Mean LAI was $3.0 (\pm 0.2, \text{SE})$ in open vs. $4.2 (\pm 0.2, \text{SE})$ in closed subplots and differed significantly between canopy treatments ($P < 0.01$; two-sample t -test). Furthermore, the resulting difference in VPD between open and closed subplots at the time of burn, $0.20 \text{ kPa} (\pm 0.06 \text{ SE})$, differed significantly from zero ($P < 0.05$; one-sample t -test). However, LMC did not differ significantly from zero between open and closed plots ($P = 0.92$; one-sample t -test).

Canopy treatment plots were then further split to $25 \text{ m} \times 12.5 \text{ m}$ subplots, 50% randomly received fuel additions. Fine leaf litter fuels were collected from

outside the experimental area and dispersed evenly across the plot. For each 25 m × 12.5 m plot, approximately 130 kg (dry weight) of fine fuels were added, or ~4.2 Mg ha⁻¹.

Prescribed fires within these split-split plots were conducted during August 27–31, 2006. Firelines were set both in the morning and afternoon, but all firelines were set at the same time for all the subplots within a whole plot. VPD (kPa) and wet weights (g) of leaf litter samples were measured at four points within each 25 m × 12.5 m fuel treatment plot immediately before the firelines were set. Samples of leaf litter were then oven-dried (65 °C for 48 h) to calculate leaf mass dry weights (g) and subsequently LMC (%). As the fire progressed through the plot, flame heights and widths (cm) were measured with rulers at five points along each active fireline at three different time intervals and then averaged for each fuel treatment plot. FSR (m min⁻¹) was calculated based on the time required to spread to the end of the plot (25 m) or on the total distance traveled. After the fire extinguished, total area burned was then mapped.

To test whether canopy opening or fuel loads had a considerable effect on fire behavior (including total area burned, flame dimensions, and FSR), analysis of variance for split plots was conducted using a linear mixed-effect model. The fuel and canopy treatments were considered fixed effects whereas the whole plot and split-plot were treated as random effects. All statistical analyses conducted with R (R Development Core Team, 2007).

Results

Initial fire behavior

In this experiment, prescribed fires were low-intensity, slow-moving surface fires typical of tropical understory forest fires (Cochrane *et al.*, 1999; van Nieuwstadt & Sheil, 2005). Initial mean flame height, flame width, and FSR (± SE) were 31 (± 1) cm, 29 (± 1) cm, and 0.21 (± 0.01) m min⁻¹, respectively. Mean initial *T* (± 56 °C resolution) measured as the fireline passed ranged from 128 °C belowground (2 cm) to 273 °C at the surface to 87 °C aboveground (100 cm).

Forest flammability decreases with repeat burns

Flame height, a proxy for fireline intensity (Rothermel & Deeming, 1980), decreased after the first burn ($P < 0.001$; ANOVA). Flame heights and widths during the second and third burns were significantly less than the first burn ($P < 0.01$; Tukey's HSD contrasts). Mean flame heights (± SE) were 33 (± 2), 24 (± 1), and 24

(± 2) cm in the first, second, and third burns, respectively. Moreover, whereas the first and second prescribed fires burned equivalent proportions of the experimental plots (i.e. mean ± SE: 79 ± 1% and 79 ± 2%), the total burned area in the third fire declined to 39 (± 2)% (Fig. 1).

Fire-induced changes in canopy structure and fuel inputs

Mean annual tree and liana mortality for the 2 years after the initial prescribed burn (≥ 10 cm DBH; *N* ~2300 individuals per plot) was 2.8 (± 0.3, % ± SE), 4.8 (± 0.5), and 5.5 (± 0.5) % yr⁻¹ after zero (B0), one (B1), and two annual burns (B3), respectively. Highest annual mortality rates during this time occurred in the 10–19.9 cm DBH size class; mean annual mortality rate (± SE) was 3.8 (± 0.9), 9.3 (± 1.3), and 9.9 (± 1.3) % yr⁻¹ in the B0, B1, and B3 plots, respectively.

Two years after the initial burn, LAI (m² m⁻²) differed significantly among all plots ($P < 0.01$; ANOVA). Mean LAI (± SE) was 5.0 (± 0.1), 4.2 (± 0.1), and 3.9 (± 0.1) in the B0, B1, and B3 plots, respectively. However, during the first 2 treatment years, mean annual litterfall did not differ across plots nor between years within the B3 plot ($P > 0.48$; ANOVA with Tukey's HSD contrasts). Mean annual litterfall (± SE) was 4.2 (± 0.1), 4.2 (± 0.1), and 4.4 (± 0.1) Mg ha⁻¹ yr⁻¹ during the first year (September 2004–August 2005) and 4.3 (± 0.1), 4.2 (± 0.2), and 4.3 (± 0.1) Mg ha⁻¹ yr⁻¹ during the second year (September 2005–August 2006) in the B0, B1, and B3 plots, respectively.

Microclimate and litter moisture content

VPD near the soil surface (~10 cm height) was indistinguishable among plots in the weeks before the first burn, but increased with repeat burns. By 2 years after the first burn, maximum daily August VPD (± SE), when many illegal burns occur, was higher in the B1 and B3 plots (2.2 ± 0.1 and 3.0 ± 0.1, respectively), compared with the control (1.8 ± 0.1). Immediately before the third set of firelines, VPD at the forest floor was significantly higher and LMC significantly lower than pretreatment conditions (Fig. 2). Mean VPD (± SE) significantly increased a year after the first and second prescribed burns compared with pretreatment levels: 2.9 (± 0.04) and 2.7 (± 0.04) vs. 2.0 (± 0.04) kPa, respectively ($P < 0.001$; ANOVA with Tukey's HSD contrasts). Mean LMC (± SE) values were similar before the first and second burns, 12.5% (± 1.0), 11.2% (± 0.4), but significantly declined to 7.7% (± 0.8) before the third burn ($P < 0.001$; Kruskal–Wallis tests).

Although the study forest presented higher VPD and lower LMC values following burning, this microcli-

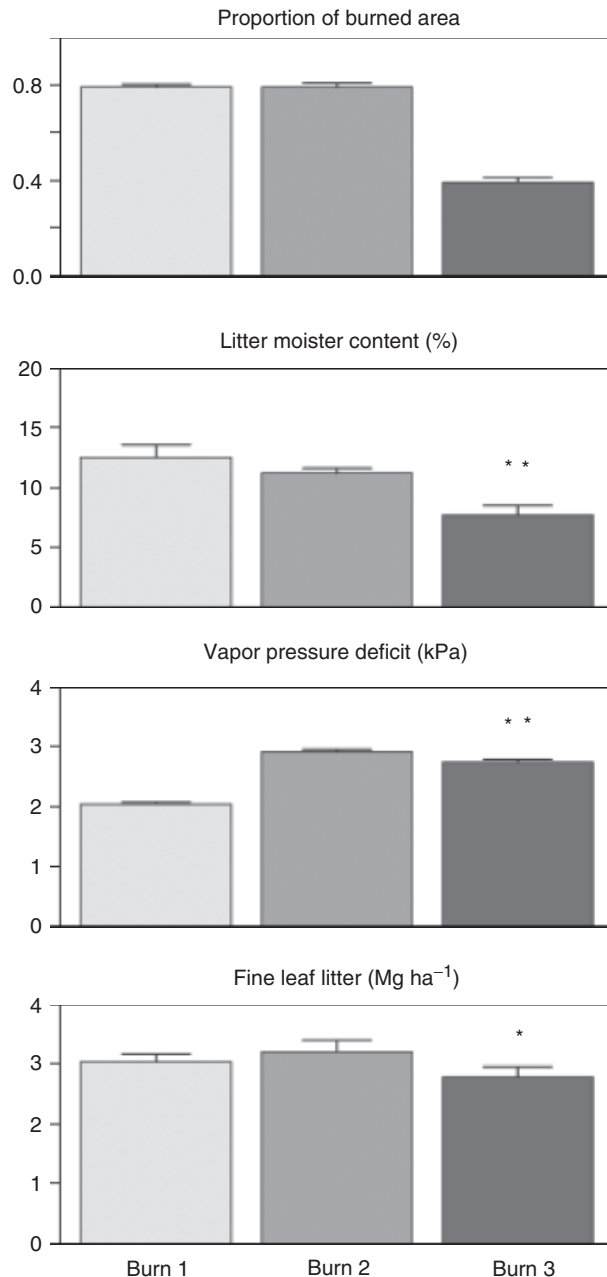


Fig. 2 Mean burned area, litter moisture content, vapor pressure deficit, and fine fuel loads (SE) before each prescribed burn (B1 and B3 plots joined for initial burn). When predictor variable before third burn is significantly different from pretreatment level, it is indicated by * ($P < 0.1$) and ** ($P < 0.001$).

matic change was not accompanied by an increase in percent of the forest floor burned or flame height. Given the 5 month period with low rainfall, the low stature of the forest canopy, and the low dry season LAI (mean SE, 4.8 ± 0.2), all of this study forest, including our control plot, appears to be microclimatically prone to burning during the severe dry season.

Fuel accumulation

Surprisingly, no significant treatment effect was found on downed fuel loads among plots, either in total fuel mass or in individual fuel size classes 2 years after initial experimental burns (Fig. 3). The hypothesis that fire would increase fuel loads was not supported.

Total downed fuel loads recovered within 11 months of each annual burn, with one notable exception; fine leaf litter did not fully recover within a year of the second fire in the B3 plot. This component of 1 h fuels significantly declined from 3.2 to 2.8 Mg ha^{-1} in 2004 vs. 2006, with a mean difference of 0.5 Mg ha^{-1} ($P < 0.1$; *t*-tests).

Two years after the initial fire, standing dead fuels in the 10–19.9 cm DBH size class significantly differed across treatment plots ($P < 0.01$; ANCOVA). They increased from $4.6 (\pm 0.9) \text{ Mg ha}^{-1}$ pretreatment to $12.4 (\pm 2.3) \text{ Mg ha}^{-1}$ after two burns (Table 1). In contrast, standing dead fuel mass did not differ in the larger size class (≥ 20 cm DBH) across plots, likely due to lower stem mortality.

Fine fuel additions

Fine fuel addition increased total burned area, FSR, and flame height and width by two to fivefold over plots without fuel additions ($P < 0.001$; linear mixed-effects model), and this effect was not influenced by subplot LAI (treefall gap vs. closed canopy). Total burned area (\pm SE) was fivefold greater in the fuel addition plots, increasing from $16 (\pm 6)\%$ to $85 (\pm 7)\%$. Also, mean FSR, flame height, and flame width (\pm SE) nearly doubled. FSR increased from $0.10 (\pm 0.01)$ to $0.18 (\pm 0.01) \text{ m min}^{-1}$, while flame height and width increased from $23 (\pm 4)$ to $42 (\pm 4) \text{ cm}$, and from $16 (\pm 2)$ to $27 (\pm 3) \text{ cm}$, respectively (Fig. 4).

Fuel consumption

Total fuel combustion (\pm SE) was $44.5 (\pm 21.2)$, $23.2 (\pm 9.1)$, and $15.3 (\pm 9.3) \text{ Mg ha}^{-1}$ in the initial, second, and third burns, respectively (Table 2). Total downed fuel consumption was similar between the first and second burns ($P = 0.88$; Kruskal–Wallis test), but significantly declined during the third burn ($P < 0.05$; Kruskal–Wallis tests). Concurrent with the declines in total fuel combustion, combustion efficiency more than halved. Only $21.7\% (\pm 10.2, \text{ SE})$ of total available downed fuels burned in 2006 compared with $50.2\% (\pm 5.7, \text{ SE})$ and $48.7\% (\pm 22.8, \text{ SE})$ in the first and second burns, respectively (Table 2).

The third fire burned substantially less fine leaf litter and 1 h fuels than the previous burns ($P < 0.001$;

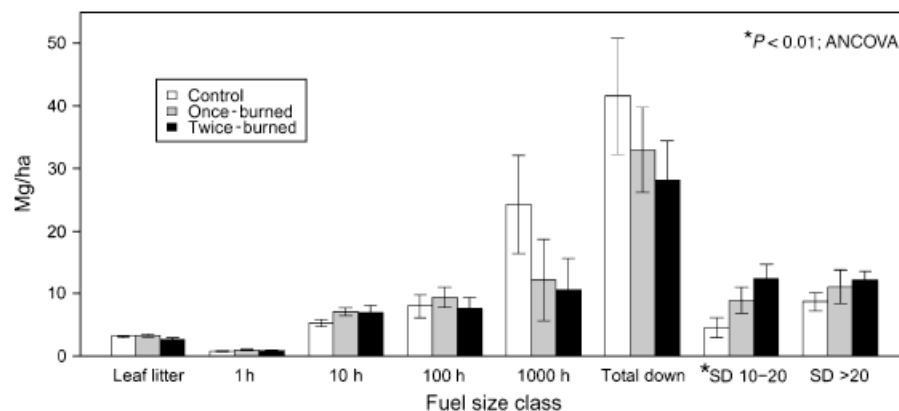


Fig. 3 Downed and standing dead (SD) fuel loads (\pm SE) across plots, 2 years after initial burn treatment. (Downed woody fuels were partitioned by moisture timelag: 1 h (0–0.6 cm diameter), 10 h (0.6–2.5 cm diameter), 100 h (2.5–7.6 cm diameter), and 1000 h (>7.6 cm diameter)).

Table 1 Mean fuel loads ($\text{Mg ha}^{-1} \pm$ SE) by size class 1 year after each prescribed fire

	Unburned 2004	Once burned 2005	Twice burned 2006
Leaf litter	3.1 (0.1)	3.4 (0.1)	2.8 (0.2)
1 h woody*	0.8 (0.1)	0.8 (0.1)	0.9 (0.1)
10 h woody	7.4 (0.6)	7.3 (0.8)	6.9 (1.1)
100 h woody	12.1 (1.7)	7.8 (1.6)	7.6 (1.9)
1–100 h (total)	20.3 (2.0)	15.9 (1.8)	15.4 (2.2)
1000 h woody	30.9 (8.6)	10.5 (3.4)	10.5 (5.0)
Total downed wood	51.3 (8.7)	26.5 (3.6)	25.3 (6.3)
Total downed fuels	55.9 (9.3)	29.9 (3.6)	28.1 (6.3)
Standing dead (10–19.9 cm DBH)	4.6 (0.9)	10.4 (1.6)	12.4 (2.3)
Standing dead (\geq 20 cm DBH)	6 (0.9)	10.2 (1.5)	12.1 (1.4)
Total necromass	68.1 (14.9)	51.2 (4.5)	53.2 (8.7)

Plots B0, B1, and B3 joined for pretreatment measure. Plots B1 and B3 joined for single burn measure, and Plot B3 represents the twice-burned measure.

*Downed woody fuels were partitioned by moisture timelag: 1 h (0–0.6 cm diameter), 10 h (0.6–2.5 cm diameter), 100 h (2.5–7.6 cm diameter), and 1000 h (>7.6 cm diameter).

DBH, diameter at breast height.

ANOVAS). The proportion of fine leaf litter combusted is approximately a third of previous burns, or $1.0 (\pm 0.3, \text{SE})$ vs. $2.2 (\pm 0.2, \text{SE})$, and $2.5 (\pm 0.3, \text{SE}) \text{Mg ha}^{-1}$ in the first and second burns, respectively.

Although significant accumulation of standing dead fuels occurs within the B3 plot, (primarily in the 10–19.9 cm DBH size class), combustion losses with repeated burns do not change in either size class ($P > 0.05$; ANOVAS). Mean combustion losses (\pm SE)

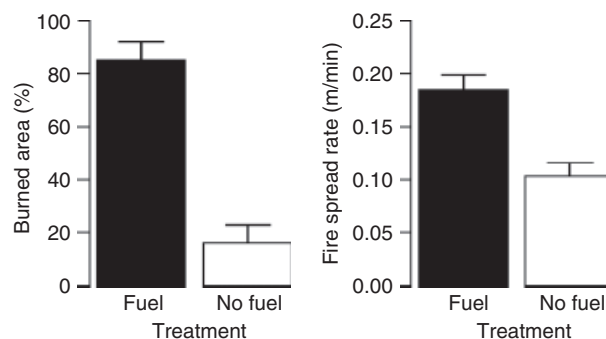


Fig. 4 Mean (\pm SE) percent burned area and FSR (m min^{-1}) in fuel/no fuel addition subplots. Both response variables significantly different between treatment subplots ($P < 0.001$; linear mixed-effects models).

were $0.1 (\pm 0.1)$, $0.7 (\pm 0.6)$, and $0.9 (\pm 0.3) \text{Mg ha}^{-1}$ in the 10–19.9 DBH size class and $0.6 (\pm 0.2)$, $1.0 (\pm 0.5)$, and $0.7 (\pm 0.5) \text{Mg ha}^{-1}$ with each consecutive burn (see Table 2). Total standing dead stems (≥ 10 cm DBH) doubled in the B3 plot between the first and third burns (from 152 to 306 standing dead stems), yet the probability of a dead stem burning during the third burn significantly declined from 12% to 3% ($P < 0.01$; logistic regression).

Discussion

We have shown that fuel loads, and fine fuels in particular, are an important determinant of fire spread in this transitional Amazonian forest. Two years after the initial burn downed fuels in all size classes are similar across once-, twice-, and never-burned plots, with an important exception. In the B3 plot, fine leaf litter fuels are replaced after one, but diminish after

Table 2 Mean combustion loss (CL; Mg ha⁻¹) and percentage fuel mass loss (\pm SE) during consecutive burns

	First burn 2004		Second burn 2005		Third burn 2006	
	CL	Loss (%)	CL	Loss (%)	CL	Loss (%)
Leaf litter	2.2 (0.2)	70.9 (4.6)	2.5 (0.3)	75.8 (5.9)	1.0* (0.3)	27.4 (11.0)
1 h woody†	0.5 (0.1)	42.5 (9.7)	0.5 (0.1)	61.4 (9.1)	-0.2* (0.2)	-58.4 (19.2)
10 h woody	2.6 (0.7)	12.2 (18.4)	2.7 (1.3)	21.1 (17.0)	1.0 (1.2)	-9.0 (16.8)
100 h woody	4.2 (1.3)	38.2 (14.3)	7.1 (3.0)	69.0 (21.3)	6.4 (1.9)	75.0 (15.3)
1–100 h (total)	7.4 (1.5)	30.8 (7.9)	10.3 (3.4)	46.9 (11.1)	7.2 (2.2)	18.6 (13.6)
1000 h	25.3 (11.5)	62.9 (9.2)	9.8 (4.3)	100.0 (0.0)	5.4 (5.2)	64.8 (22.8)
Total downed wood	33.2 (11.8)	44.5 (7.5)	20.1 (5.6)	17.2 (45.3)	11.9* (6.3)	10.8 (14.5)
Total downed fuels	37.1 (12.8)	50.2 (5.7)	22.6 (5.7)	48.7 (22.8)	12.9* (6.4)	21.7 (10.2)
Standing dead (10–19.9 cm DBH)	0.1 (0.1)	2.3 (1.5)	0.7 (0.6)	5.1 (3.7)	0.9 (0.3)	6.5 (2.4)
Standing dead (>20 cm DBH)	0.6 (0.2)	14.7 (5.8)	1.0 (0.5)	15.2 (9.2)	0.7 (0.5)	5.6 (4.2)
Total necromass	44.5 (21.2)	46.4 (5.8)	23.2 (9.1)	43.9 (17.7)	15.3 (9.3)	21.7 (10.6)

Negative value indicates fuel mass greater postfire than prefire. Plots B1 and B3 joined for 2004.

*Combustion loss differed significantly from 2004 ($P < 0.05$; ANOVA with contrasts or Kruskal–Wallis if assumptions not met).

†Downed woody fuels were partitioned by moisture timelag: 1 h (0–0.6 cm diameter), 10 h (0.6–2.5 cm diameter), 100 h (2.5–7.6 cm diameter), and 1000 h (>7.6 cm diameter).

DBH, diameter at breast height.

a second burn by $\sim 0.5 \text{ Mg ha}^{-1}$. Compared with the first and second burns, understory VPD is greater and LMC lower during the third burn, yet fires do not increase in intensity nor in burned area – as would be expected in taller, denser, seasonally dry Amazon forests (Ray *et al.*, 2005). Rather, the small decrease (by 13%) in fine leaf litter fuels may have resulted in the lower fire intensity and 50% decline in burned area during the third burn. Corroborating this conclusion, experimental fine fuel additions (increased by $\sim 4.2 \text{ Mg ha}^{-1}$) in B3 subplots doubled fire intensity and increased burned area fivefold. Because of a combination of lower fine fuel mass and less total burned area, fuel combustion emitted less carbon during the third burn, 7.7 Mg C ha^{-1} , compared with 22.3 and $11.6 \text{ Mg C ha}^{-1}$ during the first and second burns, respectively (assuming half of biomass is carbon). The reduction in flammability documented in this study highlights a fundamental principle of fire ecology – where ignition sources are present, fire propagation depends initially on available fuels and secondarily on microclimate and fuel moisture content (Whelan, 1995).

This transitional forest's flammability during the marked dry season is dependent on the rate of fuel inputs, particularly fine fuel inputs, relative to fire return intervals. Slow replacement of surface fuels may be partially explained by the following processes. First, this forest has naturally low litter production rates, half that found in central and eastern Amazon forests (4.3 vs. $7\text{--}10 \text{ Mg ha}^{-1} \text{ yr}^{-1}$; Nepstad *et al.*, 1994, 2002; Trumbore *et al.*, 1995; Salimon *et al.*, 2004; Vieira *et al.*, 2004). Second, tree and liana mortality ($\geq 10 \text{ cm}$

DBH) with one and two annual burns was low, 4.8 (± 0.5) and 5.5 (± 0.5) $\% \text{ yr}^{-1}$, 2 years after the initial burn in the B1 and B3 plots, compared with 2.8 (± 0.3) $\% \text{ yr}^{-1}$ in the control plot (B0). Other studies have found much higher fire-induced mortality rates in closed-canopy Amazon forests. For example, tree mortality ($\geq 10 \text{ cm DBH}$) was near 50%, 3 years postfire in a central Amazon forest (2000 mm yr^{-1} ; 3–5 month dry season; Barlow *et al.*, 2003; Haugaasen *et al.*, 2003), 44% 15 months postfire in an eastern Amazon forest (1750 mm yr^{-1} ; 5-month dry season; Holdsworth & Uhl, 1997), 23% 1 year postfire in a Bolivian subhumid forest (1500 mm yr^{-1} ; 3-month dry season; Pinard *et al.*, 1999), and 8% within 10 months postfire in a transitional forest $\sim 100 \text{ km}$ west of our study site (1500 mm yr^{-1} ; 5-month dry season; Ivanauskas *et al.*, 2003). Third, there may be a substantial delay in the transition of standing dead trees to available surface fuel stocks. In the B3 plot, the number of standing dead stems increased but the probability of burning declined during the third burn, suggesting that there is a stock of standing dead fuels not yet available to a low intensity fireline. These processes may explain how low rates of fuel inputs led to a negative fire feedback with an annual burning regime.

Additional negative feedback mechanisms may also be important. Beyond removing surface fuels, repeat fires may impart a longer-term negative feedback by diminishing soil nutrients (Kauffman *et al.*, 1995; Certini, 2005; Davidson *et al.*, 2007), which has been shown to limit tree growth and leaf litter production in the tropics (Vitousek, 1984; Paoli & Curran, 2007). Indeed, ≥ 5

fires reduced carbon accumulation by half in regrowing Amazon forests after clearing and burning (Zarin *et al.*, 2005). Also, fine fuel mass influences fire intensity directly and indirectly, by providing an important link in the ignition and combustion of larger, more dispersed fuels. In this transitional forest, fine fuel additions increased flame heights in previously unburned forests (J. Balch, unpublished data), and a lack of fine fuels during the third burn may have limited the ignition of increased standing dead fuels.

These results may help explain observed variation in tropical wildfires elsewhere. High tree mortality after the ENSO-related wildfires of 1997–1998 in Brazil and Indonesia, where tree mortality (≥ 10 cm DBH) was $\sim 50\%$ 3 years postfire in central Amazon forests (Barlow *et al.*, 2003) and $\sim 80\%$ 21 months postfire in East Kalimantan forests (van Nieuwstadt & Sheil, 2005), may, in part, have resulted from high fire intensity related to substantial fine fuels. The convergence of naturally high rates of litterfall production (Nepstad *et al.*, 2002; Paoli & Curran, 2007), drought-induced leaf abscission (van Nieuwstadt & Sheil, 2005), and previous logging or fire disturbance (Uhl & Kauffman, 1990; Siegert *et al.*, 2001) could make substantial fine fuels available that, in turn, increase burn intensity and severity.

Conclusions

The negative fire feedback observed in the present study, driven by low fine fuel inputs, implies that there exists a window of inflammability after multiple annual burns in these Amazon transitional forests. The combination of low, or delayed, tree mortality and low litterfall production may provide a buffer against increasing ignition sources. On the other hand, this period of inflammability may be short-lived relative to persistent anthropogenic threats (Soares-Filho *et al.*, 2006), and increasing frequency of ENSO-related droughts that, in turn, increase fuel loads (Trenberth & Hoar, 1997). A delayed wave of tree mortality and treefall due to prior fire damage, logging, and severe drought could create a pulse of available fuels. Furthermore, grass invasion from pasture or agricultural edges would create more available fine fuels (Brooks *et al.*, 2004). Moreover, although this forest is flammable during average rainfall years (Alencar *et al.*, 2006), severe drought conditions would extend the burn season and remove night-time moisture barriers to fire spread. Such a convergence of conditions could result in severe and widespread wildfires in Amazon transitional forests, which could further promote pyrophytic vegetation. Hence, the negative feedback mechanisms observed for this forest do not necessarily confer assurance that fire will not be an agent of anthropogenic change in this

region. Rather, this study demonstrates that, as the expanding soy and cattle-driven frontier further bisects the forest and leaves degraded edges, understanding fuel dynamics will be essential for predicting transitional forest flammability.

Acknowledgements

We are grateful to the Woods Hole Research Center and the Instituto de Pesquisa Ambiental da Amazônia for institutional support, in particular to the field crew at the study site; the many visiting researchers and students for assistance in carrying out the experimental fires; N. Rosa for plant identification; G. Cardinot for acquiring permits; W. Riker for data entry; and J. Reuning-Scherer for help with statistical analysis. Special thanks to Grupo Amaggi who invited this research to be conducted on their farm and provided infrastructure support. The comments of E. Davidson, U. Goodale, D. Ray, C. Runyan, D. Skelly, and two anonymous reviewers helped improve an earlier version of this manuscript. Funding for this research was provided by the David and Lucile Packard Foundation, NASA LBA-ECO program (#NCC5-700), and NSF Biocomplexity in the Environment program (#0410315). J. Balch gratefully acknowledges funding from the NSF-Graduate Research Fellowship Program, Teresa Heinz Scholars for Environmental Research program, PEO Scholar Awards program, Yale Institute for Biospheric Studies, and Yale Tropical Resources Institute, which supported her dissertation research.

References

- Alencar A, Nepstad DC, Diaz MCV (2006) Forest understory fire in the Brazilian Amazon in ENSO and non-ENSO years: area burned and committed carbon emissions. *Earth Interactions*, **10**, 1–17.
- Alencar AAC, Solórzano LA, Nepstad DC (2004) Modeling forest understory fires in an eastern Amazonian landscape. *Ecological Applications*, **14**, S139–S149.
- Barlow J, Peres CA, Lagan BO, Haugaasen T (2003) Large tree mortality and the decline of forest biomass following Amazonian wildfires. *Ecology Letters*, **6**, 6–8.
- Blate GM (2005) Modest trade-offs between timber management and fire susceptibility of a Bolivian semi-deciduous forest. *Ecological Applications*, **15**, 1649–1663.
- Bond WJ, Woodward FI, Midgley GF (2005) The global distribution of ecosystems in a world without fire. *New Phytologist*, **165**, 525–537.
- Brooks ML, D'Antonio CM, Richardson DM *et al.* (2004) Effects of invasive alien plants on fire regimes. *Bioscience*, **54**, 677–688.
- Brown JK, Oberheu RD, Johnston CM (1982) *Handbook for Inventorying Surface Fuels and Biomass in the Interior West, General Technical Report INT-129*. USDA Forest Service, Ogden, 48 pp.
- Brown S, Lugo AE (1992) Aboveground biomass estimates for tropical moist forests of the Brazilian Amazon. *Interciencia*, **17**, 8–18.
- Certini G (2005) Effects of fire on properties of forest soils: a review. *Oecologia*, **143**, 1–10.
- Chave J, Andalo C, Brown S *et al.* (2005) Tree allometry and improved estimation of carbon stocks and balance in tropical forests. *Oecologia*, **145**, 87–99.

- Clark DA, Brown S, Kicklighter DW, Chambers JQ, Thomlinson JR, Ni J (2001) Measuring net primary production in forests: concepts and field methods. *Ecological Applications*, **11**, 356–370.
- Cochrane MA, Alencar A, Schulze MD, Souza CM, Nepstad DC, Lefebvre P, Davidson EA (1999) Positive feedbacks in the fire dynamic of closed canopy tropical forests. *Science*, **284**, 1832–1835.
- Cochrane MA, Schulze MD (1999) Fire as a recurrent event in tropical forests of the eastern Amazon: effects on forest structure, biomass, and species composition. *Biotropica*, **31**, 2–16.
- Cochrane M, Skole DL, Matricardi EAT, Barber C, Chomentowski WH (2004) Selective logging, forest fragmentation, and fire disturbance. In: *Working Forests in the Neotropics: Conservation through Sustainable Management?* (eds Zarin DJ, Alavalapati JRR, Putz FE, Schmink M), pp. 310–324. Columbia University Press, New York.
- Cox PM, Betts RA, Collins M, Harris PP, Huntingford C, Jones CD (2004) Amazonian forest dieback under climate-carbon cycle projections for the 21st century. *Theoretical and Applied Climatology*, **78**, 137–156.
- Davidson EA, de Carvalho CJR, Figueira AM *et al.* (2007) Recuperation of nitrogen cycling in Amazonian forests following agricultural abandonment. *Nature*, **447**, 995–999.
- Deeming JE, Burgan RE, Cohen JD (1977) *The National Fire Danger Rating System-1978, General Technical Report INT 39*. USDA Forest Service, Ogden.
- Gerwing JJ, Farias DL (2000) Integrating liana abundance and forest stature into an estimate of total aboveground biomass for an eastern Amazonian forest. *Journal of Tropical Ecology*, **16**, 327–335.
- Grogan J, Galvão J (2006) Physiographic and floristic gradients across topography in transitional seasonally dry evergreen forests of southeast Para, Brazil. *Acta Amazonica*, **36**, 483–496.
- Hammond DS, ter Steege H, van der Borg K (2007) Upland soil charcoal in the wet tropical forests of central Guyana. *Biotropica*, **39**, 153–160.
- Haugaasen T, Barlow J, Peres CA (2003) Surface wildfires in central Amazonia: short-term impact on forest structure and carbon loss. *Forest Ecology and Management*, **179**, 321–331.
- Holdsworth AR, Uhl C (1997) Fire in Amazonian selectively logged rain forest and the potential for fire reduction. *Ecological Applications*, **7**, 713–725.
- Hurlbert SH (1984) Pseudoreplication and the design of ecological field experiments. *Ecological Monographs*, **54**, 187–211.
- Hutyra LR, Munger JW, Nobre CA, Saleska SR, Vieira SA, Wofsy SC (2005) Climatic variability and vegetation vulnerability in Amazonia. *Geophysical Research Letters*, **32**, L24712.
- INPE (2006) *Monitoring of the Brazilian Amazon forest by satellite: Project PRODES*. (<http://www.obt.inpe.br/prodes/index.html> -Accessed: June 15, 2006).
- Ivanauskas NM, Monteiro R, Rodrigues RR (2003) Alterations following a fire in a forest community of Alto Rio Xingu. *Forest Ecology and Management*, **184**, 239–250.
- Kauffman JB, Cummings DL, Ward DE, Babbitt R (1995) Fire in the Brazilian Amazon: biomass, nutrient pools, and losses in slashed primary forests. *Oecologia*, **104**, 397–408.
- Morton DC, DeFries RS, Shimabukuro YE *et al.* (2006) Cropland expansion changes deforestation dynamics in the southern Brazilian Amazon. *Proceedings of the National Academy of Sciences of the United States of America*, **103**, 14637–14641.
- Nepstad DC, de Carvalho CR, Davidson EA *et al.* (1994) The role of deep roots in the hydrological and carbon cycles of Amazonian forests and pastures. *Nature*, **372**, 666–669.
- Nepstad DC, Jipp P, Moutinho PRS, Negreiros GH, Vieira S (1995) Forest recovery following pasture abandonment in Amazonia: canopy seasonality, fire resistance and ants. In: *Evaluating and Monitoring the Health of Large-Scale Ecosystems* (ed. Rapport D), pp. 333–349. Springer-Verlag, New York.
- Nepstad DC, Moutinho P, Dias MB *et al.* (2002) The effects of partial throughfall exclusion on canopy processes, above-ground production, and biogeochemistry of an Amazon forest. *Journal of Geophysical Research – Atmospheres*, **107**, 8085, doi: 10.1029/2001JD000360.
- Nepstad DC, Verissimo A, Alencar A *et al.* (1999) Large-scale impoverishment of Amazonian forests by logging and fire. *Nature*, **398**, 505–508.
- Nepstad D, Lefebvre P, da Silva UL *et al.* (2004) Amazon drought and its implications for forest flammability and tree growth: a basin-wide analysis. *Global Change Biology*, **10**, 704–717.
- Oksanen L (2001) Logic of experiments in ecology: is pseudoreplication a pseudoissue? *Oikos*, **94**, 27–38.
- Oyama MD, Nobre CA (2003) A new climate-vegetation equilibrium state for tropical South America. *Geophysical Research Letters*, **30**, 2199–2191, doi: 10.1029/2003GL018600.
- Paoli GD, Curran LM (2007) Soil nutrients limit fine litter production and tree growth in mature lowland forest of southwestern Borneo. *Ecosystems*, **10**, 503–518.
- Pinard MA, Putz FE, Licona JC (1999) Tree mortality and vine proliferation following a wildfire in a subhumid tropical forest in eastern Bolivia. *Forest Ecology and Management*, **116**, 247–252.
- Ratter JA (1992) Transitions between cerrado and forest vegetation in Brazil. In: *Nature and Dynamics of Forest-Savanna Boundaries* (eds Furley PA, Proctor J, Ratter JA), pp. 417–429. Chapman & Hall, London.
- Ray D, Nepstad D, Moutinho P (2005) Micrometeorological and canopy controls of fire susceptibility in a forested Amazon landscape. *Ecological Applications*, **15**, 1664–1678.
- R Development Core Team (2007) *R: A Language and Environment for Statistical Computing* R Foundation for Statistical Computing, Vienna, Austria, ISBN 3-900051-07-0, <http://www.R-project.org>
- Rodríguez JP, Balch JK, Rodríguez-Clark KM (2007) Assessing extinction risk in the absence of species-level data: quantitative criteria for terrestrial ecosystems. *Biodiversity and Conservation*, **16**, 183–209.
- Rothermel RC, Deeming JC (1980) *Measuring and Interpreting Fire Behavior for Correlation with Fire Effects, General Technical Report INT-93*. USDA Forest Service, Ogden.
- Salimon CI, Davidson EA, Victoria RL, Melo AWF (2004) CO₂ flux from soil in pastures and forests in southwestern Amazonia. *Global Change Biology*, **10**, 833–843.
- Sanford RL, Saldarriaga J, Clark KE, Uhl C, Herrera R (1985) Amazon rain-forest fires. *Science*, **227**, 53–55.
- Sheil D, May RM (1996) Mortality and recruitment rate evaluations in heterogeneous tropical forests. *Journal of Ecology*, **84**, 91–100.

- Siegert F, Ruecker G, Hinrichs A, Hoffmann AA (2001) Increased damage from fires in logged forests during droughts caused by El Niño. *Nature*, **414**, 437–440.
- Soares-Filho BS, Nepstad DC, Curran LM *et al.* (2006) Modelling conservation in the Amazon basin. *Nature*, **440**, 520–523.
- Sombroek W (2001) Spatial and temporal patterns of Amazon rainfall: consequences for the planning of agricultural occupation and the protection of primary forests. *Ambio*, **30**, 388–396.
- Trenberth KE, Hoar TJ (1997) El Niño and climate change. *Geophysical Research Letters*, **24**, 3057–3060.
- Trumbore SE, Davidson EA, de Camargo PB, Nepstad DC, Martinelli LA (1995) Belowground cycling of carbon in forests and pastures of eastern Amazonia. *Global Biogeochemical Cycles*, **9**, 515–528.
- Uhl C, Kauffman JB (1990) Deforestation, fire susceptibility, and potential tree responses to fire in the eastern Amazon. *Ecology*, **71**, 437–449.
- van Mantgem P, Schwartz M, Keifer MB (2001) Monitoring fire effects for managed burns and wildfires: coming to terms with pseudoreplication. *Natural Areas Journal*, **21**, 266–273.
- van Nieuwstadt MGL, Sheil D (2005) Drought, fire and tree survival in a Bornean rain forest, East Kalimantan, Indonesia. *Journal of Ecology*, **93**, 191–201.
- Vieira S, de Camargo PB, Selhorst D *et al.* (2004) Forest structure and carbon dynamics in Amazonian tropical rain forests. *Oecologia*, **140**, 468–479.
- Vitousek PM (1984) Litterfall, nutrient cycling, and nutrient limitation in tropical forests. *Ecology*, **65**, 285–298.
- Welles JM (1990) Some indirect methods of estimating canopy structure. *Remote Sensing Reviews*, **5**, 31–43.
- Whelan RJ (1995) *The Ecology of Fire*. Cambridge University Press, Cambridge.
- Zarin DJ, Davidson EA, Brondízio E *et al.* (2005) Legacy of fire slows carbon accumulation in Amazonian forest regrowth. *Frontiers in Ecology and the Environment*, **3**, 365–369.

Supplementary material

The following supplementary material for this article is available online:

Appendix S1: Importance Value Index (IVI) for each species inventoried in overall experimental plot and each treatment sub-plot prior to burn treatment.

This material is available as part of the online article from: <http://www.blackwell-synergy.com/doi/abs/10.1111/j.1365-2486.2008.01655.x> (this link will take you to the article abstract).

Please note: Blackwell Publishing is not responsible for the content or functionality of any supplementary materials supplied by the authors. Any queries (other than missing material) should be directed to the corresponding author for the article.